View metadata, citation and similar papers at core.ac.uk

brought to you by CORE

provided by DSpace@MIT

HATSOPOULOS MICROFLUIDS LABORATORY

Department of Mechanical Engineering, Massachusetts Institute of Technology

Inductively Heated Shape Memory Polymer for the Magnetic Actuation of Medical Devices

Patrick R. Buckley, Gareth H. McKinley, Thomas S. Wilson, Ward Small IV, William J. Benett, Jane P. Bearinger, Michael W. McElfresh, and Duncan J. Maitland

February 2006
HML Report Number 06-P-05

HML@MIT
http://web.mit.edu/fluids

Inductively Heated Shape Memory Polymer for the Magnetic Actuation of Medical Devices

Patrick R. Buckley, Gareth H. McKinley, Thomas S. Wilson, Ward Small IV, William J. Benett, Jane P. Bearinger, Michael W. McElfresh, Duncan J. Maitland

Abstract

Presently there is interest in making medical devices such as expandable stents and intravascular microactuators from shape memory polymer (SMP). One of the key challenges in realizing SMP medical devices is the implementation of a safe and effective method of thermally actuating various device geometries *in vivo*. A novel scheme of actuation by Curie-thermoregulated inductive heating is presented. Prototype medical devices made from SMP loaded with Nickel Zinc ferrite ferromagnetic particles were actuated in air by applying an alternating magnetic field to induce heating. Dynamic mechanical thermal analysis was performed on both the particle-loaded and neat SMP materials to assess the impact of the ferrite particles on the mechanical properties of the samples. Calorimetry was used to quantify the rate of heat generation as a function of particle size and volumetric loading of ferrite particles in the SMP. These tests demonstrated the feasibility of SMP actuation by inductive heating. Rapid and uniform heating was achieved in complex device geometries and particle loading up to 10% volume content did not interfere with the shape recovery of the SMP.

I. INTRODUCTION

Shape memory polymers (SMPs) are a class of polymeric materials that can be formed into a specific primary shape, reformed into a stable secondary shape, and then controllably actuated to recover the primary shape. A review of SMP basics and representative polymers was given by Lendlein [1]. The majority of SMPs are actuated thermally, by raising the temperature of the polymer above the glass (or crystalline) transition of the matrix phase. Typically, through this transition the modulus decreases from that characteristic of the glassy state (~10^9 Pa) to that of an elastomer (~ 10^6 to 10^7 Pa). Upon cooling, the original modulus is almost completely recovered and the primary form is stabilized. While other classes of thermally activated shape

memory materials have been developed, shape memory alloys (SMA) [2] and shape memory ceramics [3] being the two other major classes [4], SMPs have a number of unique and promising properties. Specifically, in the field of medicine, research into the development of new SMP with adjustable modulus [5], greater strain recovery, an adjustable actuation temperature, and the option of bioresorption [1, 6] has opened the possibility for new medical devices and applications.

Some SMP devices that are being researched presently include an occlusive device for embolization in aneurysms [7], a microactuator for removing clots in ischemic stroke patients [8, 9], a variety of expandable stents with drug delivery mechanism [10, 11], cell seeded prosthetic valves [11], and self tensioning sutures [1]. One of the key challenges in realizing SMP medical devices is the design and implementation of a safe and effective method of thermally actuating a variety of device geometries *in vivo*. When the soft phase glass transition temperature of the SMP is above body temperature, an external heating mechanism, usually photothermal (laser heating) or electrical (resistive heating) is required [8]. A novel alternative to these traditional methods of actuation is inductive heating: loading ferromagnetic particles into the SMP and exposing the doped SMP to an alternating magnetic field to cause heating.

The use of magnetic particles and an applied magnetic field has a variety of potential advantages over traditional methods of actuation. One of the key advantages is the innate thermoregulation offered by a ferromagnetic material's Curie temperature (T_c). T_c is the temperature at which a ferromagnetic material becomes paramagnetic, losing its ability to generate heat via a hysteresis loss mechanism [12]. By using particle sizes and materials that will heat mainly via a magnetic hysteresis loss mechanism instead of an eddy current mechanism, it becomes possible to have an innate thermoregulation mechanism that limits the maximum achievable temperature to T_c. By selecting a ferromagnetic particle material with a T_c within safe medical limits, Curie thermoregulation eliminates the danger of over heating and the need for a feedback system to monitor device temperatures. Other benefits of the inductive heating approach are the following:

1. Power transmission lines leading to a SMP device are eliminated. Eliminating fiber optics and wires and the connection of these items to a device simplifies design and eliminates a possible point of failure.
2. More complex device shapes are possible. Provided that uniform distribution of the magnetic particles is achieved, the conduction lengths are short and consistent and consistent heating is expected for any type of device geometry, whereas traditional laser and electro-resistive heating methods impose constraints on device geometry due to the requirement of correct light refraction/absorption and thermal conduction through the device geometry.
3. Selective heating of specific device areas is possible by impregnating only the desired areas with magnetic particles. This scheme, in effect, allows a device to have a variable modulus from location to location in the device, introducing a new design variable and the possibility for new types of devices.
4. Remote actuation allows for the possibility of implantable devices that can be later actuated by an externally applied magnetic field, opening the possibility for an entirely new class of SMP devices such as tissue scaffolds for tissue regeneration.

The use of medically-safe magnetic fields to selectively heat Curie thermoregulated ferromagnetic materials *in vivo* to temperatures of $\geq 42°C$, has been demonstrated in a number of hyperthermia studies [13-18] suggesting the feasibility of the same approach to actuate SMP devices *in vivo*. The impact of particle size and material processing on the magnetic loss mechanisms and heating characteristics of magnetic particles is quite complicated but is fairly well understood thanks to previous research [19, 20]. Theories have been developed that allow analytical techniques to optimize particle size and processing to maximize heating for a specified amplitude and frequency magnetic field [21, 22]. In fact, particle sizing and material processing to optimize heating characteristics in medically-safe magnetic fields for biocompatible magnetite materials has already been laid out in research done on Magnetic Fluid Hyperthermia (MFH) [19,

21, 23]. If anything these previously-reported magnetite particles heating efficiencies are overly optimized for an SMP application as it will be possible to have higher concentrations of particles in the SMP than it is possible to achieve in cancerous cells, which must be enticed to take up the particles and are only expected to have particle concentrations of roughly 15 mg Fe/g [24]. Unfortunately these magnetite-based MFH particles that have been optimized for heating efficiency are not optimized for Curie thermoregulation, which is a desired property for particles used in an SMP application.

Materials tailored to have a Curie temperature in the physiologically useful range have been developed [25], but are often less biocompatible then the magnetite materials previously mentioned. However, the biocompatibility requirements of particle materials used in an SMP application are expected to be less stringent than those used for MFH as the particles embedded in the SMP will not be in direct contact with biological tissue. This opens the possibility of using a wider range of magnetic materials.

In this work, Nickel Zinc ferrite particles were used to achieve SMP actuation by inductive heating. Prototype SMP medical devices made from Nickel Zinc ferrite loaded SMP were thermally actuated in air using a 12.2 MHz magnetic field to demonstrate feasibility of the inductive heating approach. The effect of volumetric particle loading from 1% to 20% on the heating efficiency of the magnetic particles was also investigated. Dynamic mechanical thermal analysis (DMTA) was used to assess the change in mechanical properties of the SMP with the addition of particles at 10% volume content.

II. MATERIALS AND METHODS

A. Magnetic Particles

Nickel zinc ferrites are one class of material that shows promise for an inductively heated SMP application. Research into the use of inductively-heated particles for the bonding and curing of thermoplastics has already demonstrated that Nickel Zinc Ferrites can have variable Curie temperature through zinc substitution, as shown in Fig. 1, as well as the ability to achieve self-

thermoregulation via a Curie hysteresis mechanism[26]. Besides having an adjustable Curie temperature, Nickel Zinc ferrites have other material properties that make them well-suited to the proposed SMP application. They have a high electrical resistivity, on the order of 10^6 to 10^{10} Ohm-cm, this serves to minimize eddy current heating [26] allowing heat to be generated mainly via hysteresis losses. They are also environmentally stable, making it less likely that the particles will react with the polymer material.

Three compositions of Nickel Zinc Ferrites were obtained from Ceramic Magnetics Inc.: C2050, CMD5005, and N40. This nomenclature is provided by the manufacturer and does not indicate any specific material composition or concentration. These particles were reported by the manufacturer to have an average size of roughly 50 microns and a spherical shape. Particles were sorted further using 53μm, 43μm, 25μm, 16μm, and 8μm pore screen meshes and some material was also ball-milled to obtain even smaller particles. Image analysis was used to classify particle size. Three different average sizes were obtained: 43.6μm, 15.4μm, and 6.7 μm. The 6.7 μm particles were produced from a 5 hour ball milling process. Pertinent properties of these materials, including Curie temperature, are listed in Table I.

B. Magnetic Field Generation

The induction heating equipment used for initial testing was an Ameritherm Nova 1M power supply with a remote heat station, and a copper-wound solenoid coil with a 2.54cm diameter, 7.62cm length, and a total of 7.5 turns. This unit had an adjustable power setting capable of outputting 27 to 1500 Watts at between 10 and 15 MHz frequency. This high frequency would likely induce eddy currents in tissue [13], causing undesirable direct heating of the human body in medical applications. While the high frequencies used here are not suitable for direct clinical use the same magnetic loss mechanisms present at the clinically usable frequencies, 50 kHz -100 kHz [27], should also be present in the particle materials at the higher frequencies used here, albeit at a different quantitative level. For these reasons the 10-15 MHz range was seen as suitable for proof-of-principle testing.

The magnetic field was calculated indirectly using measurements of the impedance and the voltage drop across the coil. A Hewlett Packard 4285A 75 kHz-30 MHz LCR meter was employed to measure the impedance, which was (525 ± 7.2) nH at a frequency of 12.96 MHz. Assuming that the electrical resistance of the copper coil was negligible compared to the resistance created by the inductive reactance, it becomes possible to calculate the current through the coil using the following equations:

$$2\pi fL = X_L \quad \textbf{(1)}$$

$$\frac{V}{X_L} = i \quad \textbf{(2)}$$

where L is the impedance in Henry (525 nH), f is the frequency in Hz as measured using an oscilloscope, X_L is the inductive reactance, V is the rms voltage in volts as measured using an oscilloscope, and i is the calculated current in Amps. Assuming the coil can be modeled as an ideal solenoid the magnetic field at the center of the coil can be described as follows according to the Biot-Savart law [28],

$$\frac{\mu_o N i}{\sqrt{(4R^2 + L^2)}} \times \frac{10^7}{4\pi} = H \quad \textbf{(3)}$$

where μ_o is the permeability of free space and is equal to $4\pi \times 10^{-7}$ Henry/meter, N is the number of turns in the coil, i is the current through the coil in amps, R is the coil radius in meters, L is the coil length in meters, $\frac{10^7}{4\pi}$ is a conversion factor, converting from units of Tesla to A/m, and H is the field strength in A/m. Using the above techniques the peak magnetic field strength at the center of the coil was calculated for several power settings , this information is presented in the calibration curve found in Fig. 2. This calibration curve is not linear due to the reflected power in the circuitry of the Ameritherm equipment [29].

C. Prototype Device

To determine the impact of the added magnetic particles on SMP shape recovery, a proof-of-principle test was conducted to evaluate the actuation of complex shaped devices made using ferromagnetic particle loaded SMP. Two prototype therapeutic devices currently being developed in-house that would be difficult to heat and actuate using laser or resistive heating techniques due to their complex geometries were chosen: a flower-shaped endovascular thrombectomy device for stroke treatment and an expandable SMP foam device for aneurysm embolization. These devices are shown in their collapsed and deployed forms in Fig. 3. These devices and mechanical test samples were made from an ester-based thermoset polyurethane SMP, MP 5510, purchased from Diaplex Company Ltd., a subsidiary of Mitsubishi Heavy Industries, Ltd. The Diaplex SMPs are segmented polyurethanes whose morphological structure is bi-phasic, consisting of a soft phase matrix with hard phase inclusions. Actuation is achieved by heating above the soft phase transition; the nominal soft phase glass transition temperature of MP 5510 is 55°C. The SMP was loaded with 10% by volume C2050 43.6 micron diameter Nickel Zinc Ferrite particles. The devices were exposed to an alternating magnetic field of 12.2 MHz and approximately 400 A/m (center of the inductive coil) in air at room temperature while an infra-red thermal imaging camera recorded device temperature during actuation.

D. Dynamic Mechanical Thermal Analysis (DMTA)

To quantify the impact of the nickel zinc ferrite particles on the mechanical properties of the SMP, a DMTA test was conducted on neat SMP and particle loaded SMP. Testing samples were prepared using the same SMP, particles, and particle concentrations used in the prototype devices previously described. Measurements were made using a TA ARES-LS2 model rheometer with TA Orchestrator control software. The test atmosphere was dry air with heating by forced convection. Samples were first prepared by polymerizing in 1 ml syringes (polypropylene) at manufacturer recommended conditions [30]. Resulting samples were typically 4.65 mm in diameter and up to 70 mm in length. The ARES instrument was set up with a torsion cylinder test fixture and the test geometry typically used was at the molded diameter and with a 25 mm gap

between upper and lower fixtures. Dynamic strain sweeps at temperature extremes (25 and 120 C) were used to determine the range of linear viscoelastic behavior of the neat polymer. Dynamic temperature sweep tests were then performed on all samples at 6.28 radians/second (1 Hz) frequency from 25 to 120 ˚C, at a constant heating rate of 1˚C/minute, and starting with a shear strain of 0.01% while using the control features of the software to adjust strain upward as temperature increased to maintain a minimum torque of 2 gram-cm. Data points were collected every 15 seconds. The rheological quantities of dynamic shear storage modulus G', dynamic shear loss modulus G", and the loss ratio tan δ (=G"/G') were calculated by the Orchestrator software from the raw torque and angular displacement data using standard formulae [31].

E. Curie Thermoregulation and Hysteresis Loss

The presence of eddy current loss mechanisms in the inductive heating process can overcome the mechanism of thermoregulation offered by the Curie temperature limit imposed by hysteresis loss. Therefore, if temperatures above the particle Curie temperature can be reached in a given applied magnetic field, eddy current loss exists. The presence of eddy current loss was determined by using flakes of various Omega Marker temperature sensitive waxes mixed with the nickel zinc ferrite particles and then heated in a 12.2 MHz 545 A/m magnetic field. The thermo-sensitive wax transitions rapidly from a solid to a liquid at a prescribed temperature making it possible to determine when the particles had reached a specific temperature by physical observation.

F. Calorimetry Tests

A calorimeter was made using a 2.54cm diameter Styrofoam cylinder. A 1.27cm hole was bored through the center of the Styrofoam to accommodate a 1.27cm diameter plastic test tube filled with 4 ml of double distilled deionized water. A Styrofoam top was fashioned to cover the exposed top of the test tube. This testing setup is illustrated in Fig. 4. This configuration left a 6.35mm thick wall of insulating Styrofoam around the entire test tube. To check that this was sufficient to prevent discernable heat loss to the environment a heat transfer calculation for the

calorimeter geometry was conducted. The convective heat transfer coefficient for the calorimeter geometry of the calorimeter with free air convection was calculated to be h = 4.507 W/m^{2}K. Using this value, the time for the system to reach 95% of its steady state temperature, meaning the inflow of heat is approximately equal to the outflow, was calculated to be 464.4 seconds. This value is an order of magnitude greater than the time of the longest test, which was 45 seconds, suggesting that heat loss over the course of the tests was negligible.

SMP calorimetry samples were 1 mm thick discs with a diameter of 9.52mm. Twelve different MP 5510 SMP samples with varying magnetic particle sizes, volume content, and material types were prepared and tested. A SMP disc of the same geometry as the other samples but with no magnetic particles was also tested to serve as a control.

Samples were loaded into the Styrofoam calorimeter so they were centered in the inductive coil. The sample position in the coil was consistent for all tests to ensure that all samples experienced the same magnetic field. An alternating magnetic field of 12.2 MHz and prescribed field strength was then applied for a designated amount of time. Immediatly after the field was turned off, the temperature rise of the water was measured using a thermocouple. Temperature was not measured during magnetic field exposure because the thermocouple would have been directly heated by the magnetic fields used.

Tests were performed at a power setting of 500 and 1000 Watts on the Ameritherm power supply, and at 10, 20, 30, and 45 second exposure times. These power settings correspond to peak field strengths of (422 ± 35) A/m and (545 ± 45) A/m as calculated using equations 1, 2 and 3 (see calibration curve in Fig. 2). Temporal heating curves (temperature change as a function of magnetic field exposure time) were generated by averaging three temperature measurements at each time setting, a representative set of these curves is shown in Fig. 5.

Using the temperature rise measured in this series of tests a power dissipation rate for each sample was calculated. It was assumed that the mass of the sample disc had negligible effect on the thermal properties of the system since the sample disc was less than 3%, by mass or

volume, of the 4 ml of water. Using this assumption and neglecting any heat loss to the environment, the power generated in each test is equal to the power needed to heat the 4ml of water. This allows the power dissipation to be calculated using the following equation:

$$\rho_w c_p v_w \frac{dT}{dt} = P_g \quad \textbf{(4)}$$

where ρ_w is the density of water in units of g/cm^3 (0.99823 g/cm^3), c_p is the specific heat of water in units of J/gK (4.182 J/gK), v_w is the volume of water in units of cm^3 (4 cm^3), *dT/dt* is the rate of temperature rise of the water in units of K/s (calculated from the slope of the heating curves), and P_g is the dissipation in Watts. P_g was divided by the sample volume, 0.07118 cm^3, to derive the average volumetric power dissipation of the inductively heated SMP samples. The volumetric power dissipation of the magnetic particles was also calculated by first subtracting the P_g of the neat SMP control sample from that of the particle loaded samples and then dividing this adjusted P_g by the volume of the magnetic particles.

III. RESULTS

A. Prototype Device Actuation

Thermal images of the SMP devices actuating are shown in Fig. 6. Both the flower and foam devices fully actuated, showing qualitatively that the presence of particles up to 10% by volume did not interfere with the shape memory properties of the material. The flower actuated in under 25 seconds, with the magnetic field elevating the temperature of the device from 23˚C to 64˚C. The foam actuated in under 15 seconds with the temperature rising from 23˚C to over 78.6˚C. Neither particle volume content nor magnetic materials were optimized for either of the devices.

B. Dynamic Mechanical Thermal Analysis (DMTA)

The glass transition temperature of the SMP and the ratio of glass state to rubber plateau moduli have been used previously to characterize the SMP actuation temperature and shape

recovery properties of SMPs [32, 33]. DMTA was used to determine these properties for particle-loaded and neat (unloaded) SMP, with storage and loss moduli G' and G" shown in Fig. 7. Values of Tg, as well as the storage moduli (G') at T_g -20˚C, and at T_g+20˚C were calculated from the data and are given in Table II. While either the peak in G" or the peak in tanδ are often used to define Tg, the average temperature of the two peaks is used to determine Tg here. This average in peak temperature is closer to the midpoint in the transition from the glassy state modulus to the rubber plateau modulus for these materials. The maximum in loss modulus and loss tangent that occur during DMTA tests signal different degrees of molecular motion in the polymer, with the maximum in the loss modulus signaling shorter range motion associated with the onset of the glass transition region, and the maximum of the loss tangent signaling longer range coordinated molecular motion associated with approaching the end of the glass transition region and the beginning of the rubbery plateau region [33]. All of these values increased with the addition of particles.

C. Curie Thermoregulation

Using the thermo-sensitive waxes to gauge the temperature of the Nickel Zinc ferrite particles, CMD5005 and C2050 were observed to stop heating at close to their nominal Curie temperatures of 130˚C and 340˚C, respectively. The Curie temperature of N40 (510˚C) was beyond the temperature range of the Omega Marker waxes but it was observed to heat above 340˚C as expected. While these temperatures may exceed acceptable physiological limits the results demonstrate the nature of Curie thermoregulation, and they suggest that the magnetic heating mechanisms at work are those of hysteresis losses and not eddy currents at the applied field of 12.2 MHz and 545 A/m. Further, theoretical predictions of eddy current power dissipation in conductive particles show a direct proportionality with the square of the frequency of the applied field and the diameter of the particle [34], suggesting that the use of lower frequencies and smaller particles would even further reduce the presence of eddy currents, thereby maintaining and even enhancing the Curie thermoregulation mechanism.

D. Calorimetry Tests

Representative temporal heating curves for SMP loaded with a specific particle type and size (C2050, 43.6 micron) as well as for neat (unloaded) SMP are shown in Fig. 5. Volumetric power dissipation of nickel zinc ferrite particles between 6.7 and 43.6 microns diameter was demonstrated to be between 128-1050 W/cm^3 for a 12.2 MHz magnetic field strength of 422-545 A/m, as shown in Table III. The observed decrease in power dissipation as particle diameter decreased was a predictable result according to multidomain magnetic particle theory that shows coercivity to be proportional to the inverse of the diameter [21]. Also, basic magnetic hysteresis theory predicts the observed increase in power dissipation for multidomain magnetic particles at increasing magnetic field strengths when field amplitudes are below the material coercivity [35], as is the case in these tests. An interesting and unexpected trend that is present in the calorimetry data is a decrease in the particle heating efficiency as the volume content of particles increases. This trend was present for both field strengths, 545 A/m and 422 A/m, and can be seen in the 545 A/m data in Fig. 8. The volumetric power dissipation of the magnetic particles in SMP at 20% volume fraction was roughly 40% less than that at 1% volume fraction.

IV. DISCUSSION

While the high Curie temperature of the magnetic particles and frequency of the magnetic fields used here are not optimized for medical use, clinically safe magnetic fields have been used to selectively heat Curie thermoregulated ferromagnetic materials *in vivo* to clinically relevant temperatures of $\geq 42°C$ in a number of hyperthermia studies [13-18], suggesting the feasibility of the same approach to actuate SMP devices *in vivo*. It is also possible that particles used in the inductive heating of SMP will have less stringent biocompatibility requirements than those materials used in hyperthermia since the particles will be encased in SMP and will not directly interact with human tissue, opening the potential of using a wider range of magnetic materials. For these reasons it should be easy to find a suitable particle material that heats with clinically

safe magnetic fields. However questions about how particles interact with the SMP matrix and how their dispersion and proximity to one another affect heating characteristics remain.

The observed decrease in the volumetric heating efficiency of particles as volume content of particles in SMP increased points to a possible magnetic shielding effect the particles may have on each other as they become more closely packed in the polymer matrix. This shielding could lower the magnetic field strength experienced by the particles and thus lower the volumetric power dissipation. No previous research on this effect has been found, making it a possible topic for further work. While the diminished heating efficiency of particles at higher volume contents is something to be aware of, it does not appear that it will prevent SMP actuation as sufficient heating for SMP actuation occurred at relatively low particle concentrations of five to ten percent by volume.

The effect of particulate filler on a continuous polymer matrix has been previously studied in great detail and a number of models exists which can predict the impact of particles on the shear modulus of the composite [36]. The DMTA results can be compared to these theoretical predictions in order to provide a sense of how closely the inductively heated SMP material conform to classical expectationss. One well known model is the Guth and Smallwood equation [36]:

$$G = G_m(1 + 2.5\phi + 14.1\phi^2) \quad \textbf{(5)}$$

where G is the shear modulus of the polymer/particle composite, G_m is the matrix modulus taken to be that of the neat polymer, and ϕ is the volume fraction of particles. Equation 5 predicts that the presence of 10% volume of particles should increase the modulus by roughly 39%. The observed results were close to this, with the glassy modulus of the material increasing by 56%, and the rubbery modulus by 24%. More extensive DMTA testing is in progress to further characterize the affect that different particle volume contents have on the mechanical properties of the SMP.

V. CONCLUSION

We have demonstrated the feasibility of fabricating inductively-heated SMP devices employing dispersed nickel zinc ferrite ferromagnetic particles and using a magnetic field to trigger actuation. Elimination of a physical power connection removes restrictions on device geometry imposed by laser and resistive heating modalities. Furthermore, as a result of the predominant hysteresis loss heating mechanism, self-thermoregulation can be achieved by tailoring the particle Curie temperature to prevent overheating in medical applications. Initial actuation testing indicated that the addition of 10% volume content of particles provides sufficient heating for SMP actuation in air and does not interfere significantly with the shape memory properties of the material. Preliminary DMTA results show an increase in the modulus of the SMP composite with the addition of 10% particles, that is in accordance with standard composite theory as well as an increase in the glass transition temperature of the soft phase of the SMP. With further optimization of particle material to provide clinically acceptable Curie temperatures and magnetic field frequencies, inductive heating may provide an effective means of deployment of SMP medical devices.

ACKNOWLEDGMENT

This work was performed under the auspices of the U.S. Department of Energy by Lawrence Livermore National Laboratory under Contract W-7405-ENG-48 and supported by the National Institutes of Health/National Institute of Biomedical Imaging and Bioengineering, Grant R01EB000462.

TABLE I
MAGNETIC AND MATERIAL PROPERTIES OF NICKEL ZINC FERRITE PARTICLES

	C2050	CMD5005	N40
Initial Permeability	100	1600	15
Max Permeability	390	4500	50
Max Flux Density* (Gauss)	3400	3000	1600
Remnant Flux Density* (Gauss)	2400	1800	700
Coercive Force* (A/m)	239	18	597
Curie Temperature (˚C)	340	130	510
Density (g/cm^3)'	5.57	6.16	5.65
Resistivity (Ohm-cm)	10^6	10^9	10^{10}

*Measurement reported by manufacturer at 3184 A/m applied field strength
†Measurement made by authors (not provided by manufacturer)

TABLE II
DMTA RESULTS FOR PARTICLE LOADED SMP COMPARED TO NEAT (UNLOADED) SMP

Volume (%), Particle Diameter (µm), Material	G'(Tg-20C) (MPa)	G'(Tg+20C) (MPa)	T_g (˚C)
10%, 43.6µm, C2050	1010	4.85	61.4
0%, neat SMP	646	3.09	55.5

TABLE III
VOLUMETRIC POWER DISSIPATION OF MAGNETIC PARTICLES AND AVERAGE VOLUMETRIC POWER DISSIPATION OF SAMPLES FOR 12.2 MHz AND 422 A/m AND 545 A/m MAGNETIC FIELDS

		Volumetric Power Dissipation of Magnetic Particles (W/cm^3)		Average Volumetric Power Dissipation of Samples (W/cm^3)	
Magnetic Material	**Volume %, Particle Diameter**	**422 A/m Field**	**545 A/m Field**	**422 A/m Field**	**545 A/m Field**
C2050	1, 6.7 μm	208	566	2.1	5.7
C2050	1, 43.6 μm	500	1050	5.0	10.5
C2050	5, 6.7 μm	240	518	12.0	25.9
C2050	5, 43.6 μm	414	803	20.7	40.1
C2050	10, 6.7 μm	177	407	17.7	40.7
C2050	10, 15.4 μm	338	717	33.8	71.7
C2050	10, 43.6 μm	356	783	35.6	78.3
C2050	20, 6.7 μm	128	300	25.6	60.0
C2050	20, 43.6 μm	268	593	53.6	118.6
N40	10, 43.6 μm	278	495	27.8	49.5
CMD5005	10, 43.6 μm	296	503	29.6	50.3
None (neat SMP)	N/A	N/A	N/A	4.0	6.0

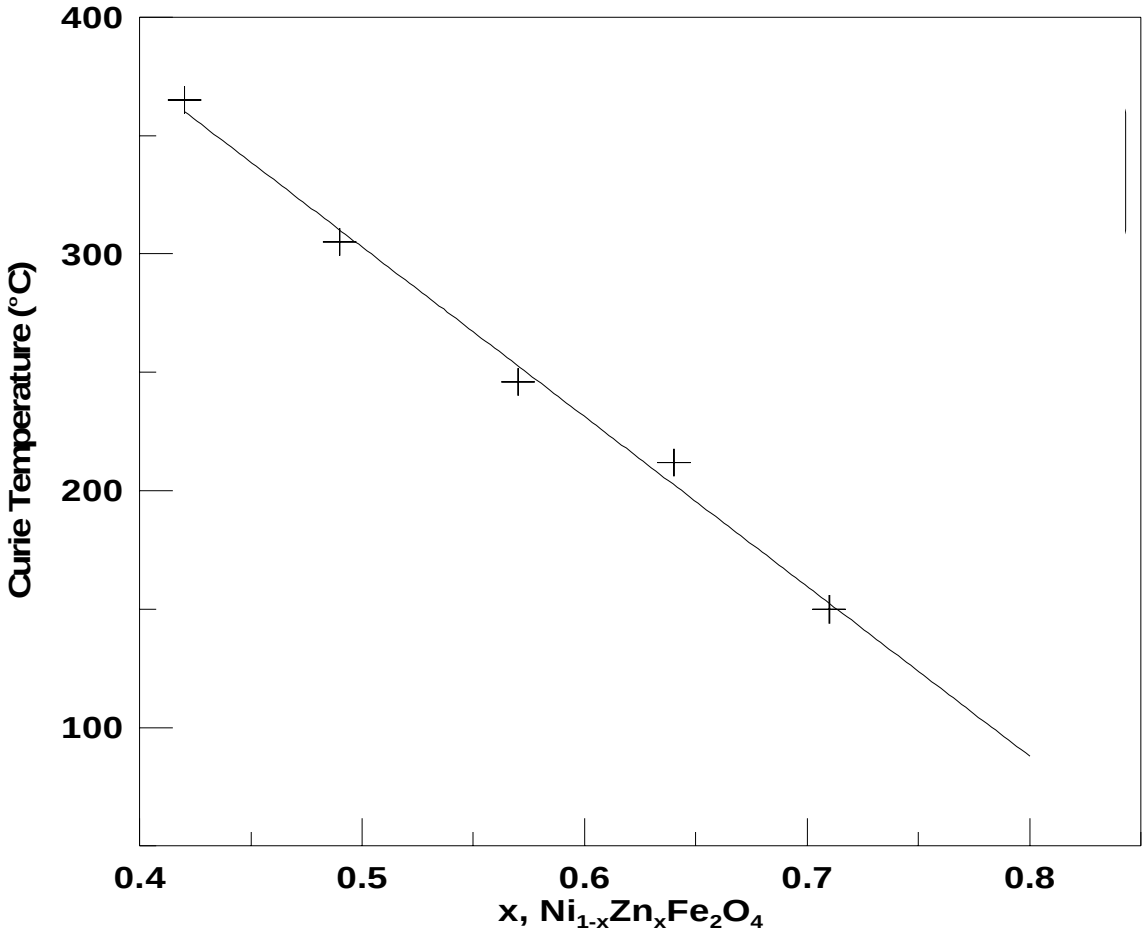
400
300
200
100
Curie Temperature (°C)
0.4
0.5
0.6
0.7
0.8
x, Ni1-xZnxFe2O4

Fig. 1

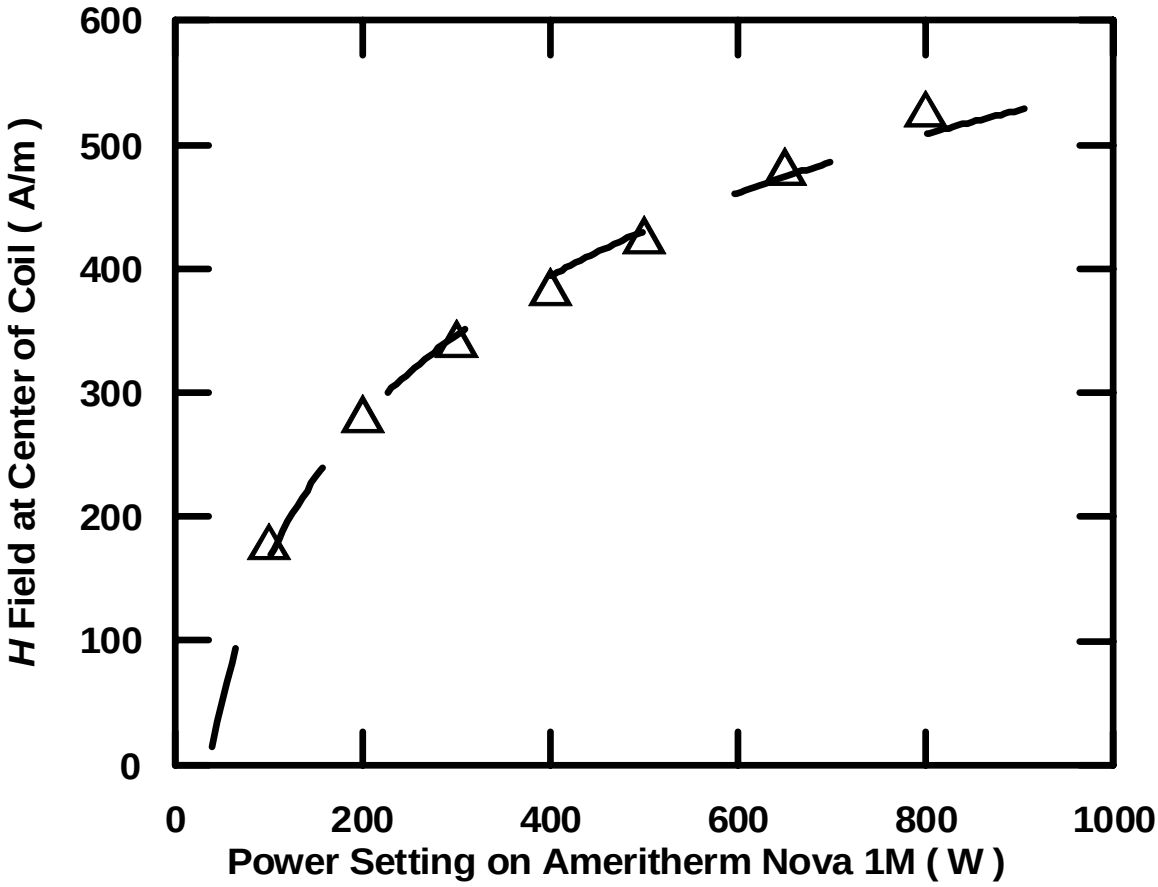
600
500
400
300
200
100
0
H Field at Center of Coil (A/m)
0
200
400
600
800
1000
Power Setting on Ameritherm Nova 1M (W)

Fig. 2

a)

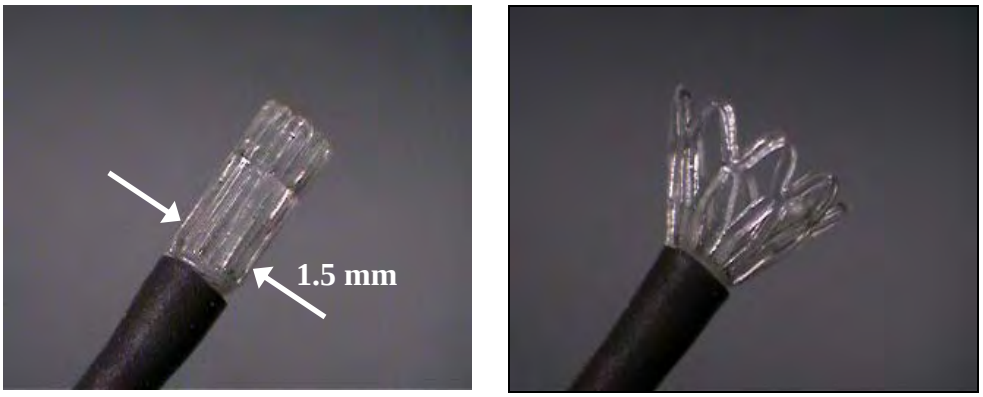

b)

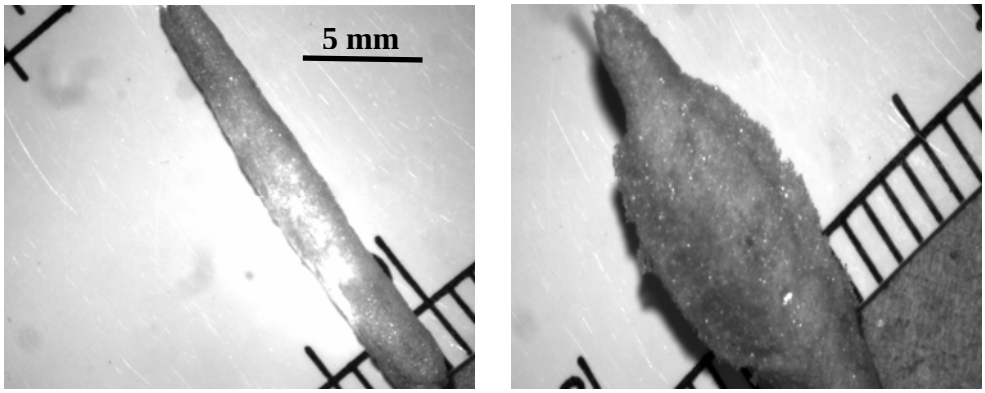

Fig. 3

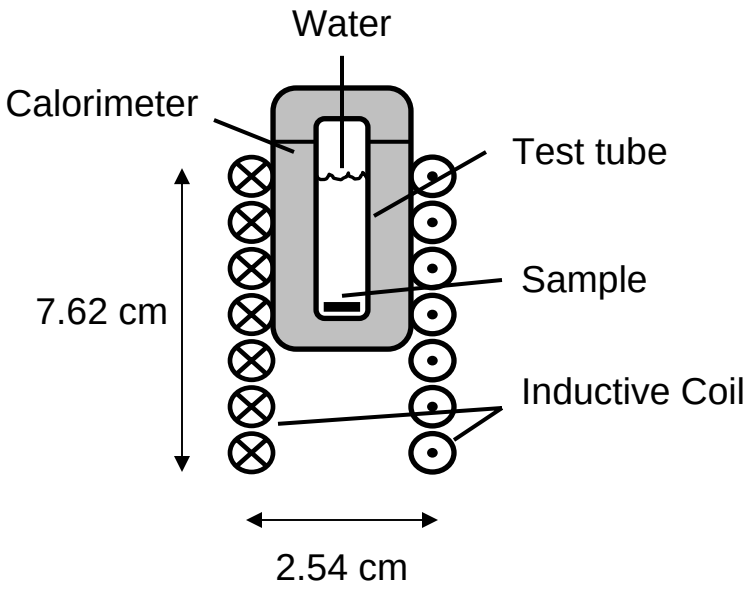
Water
Calorimeter
Test tube
Sample
7.62 cm
Inductive Coil
2.54 cm

Fig. 4

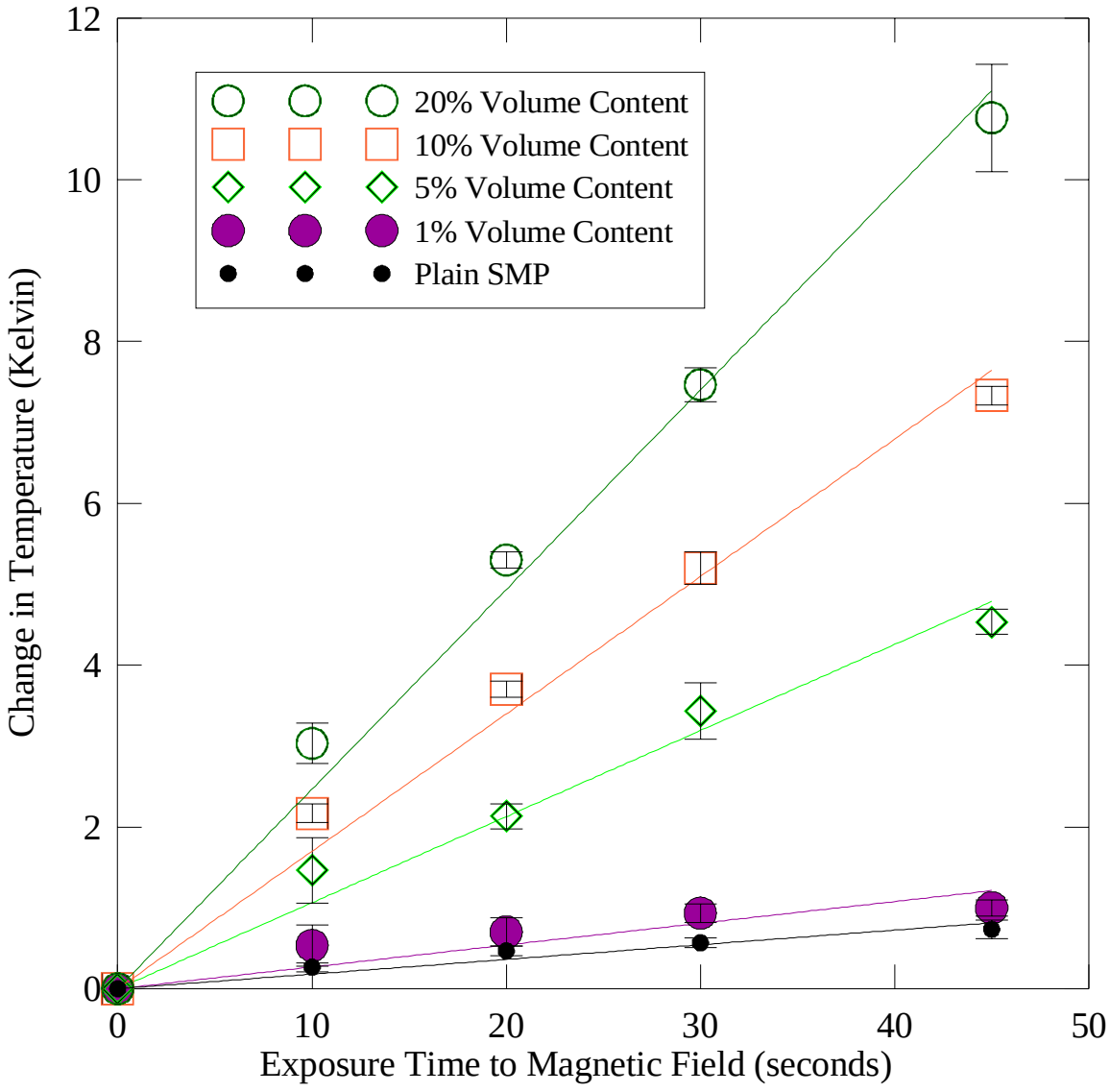
20% Volume Content
10% Volume Content
5% Volume Content
1% Volume Content
Plain SMP
Change in Temperature (Kelvin)
Exposure Time to Magnetic Field (seconds)
0
2
4
6
8
10
12
0
10
20
30
40
50

Fig. 5

a)

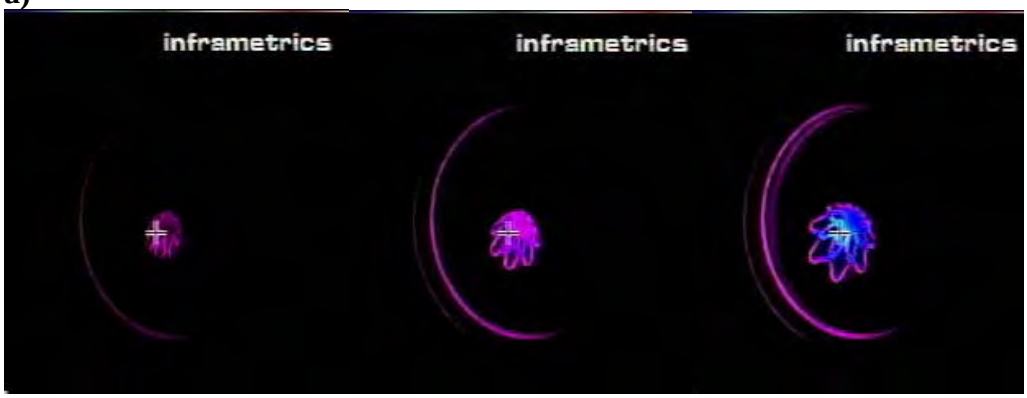
inframetrics
inframetrics
inframetrics

b)

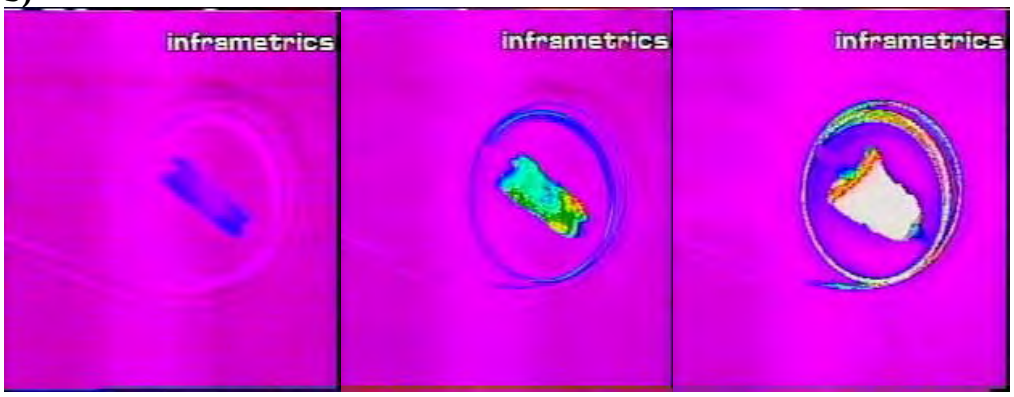
inframetrics
inframetrics
inframetrics

Fig. 6

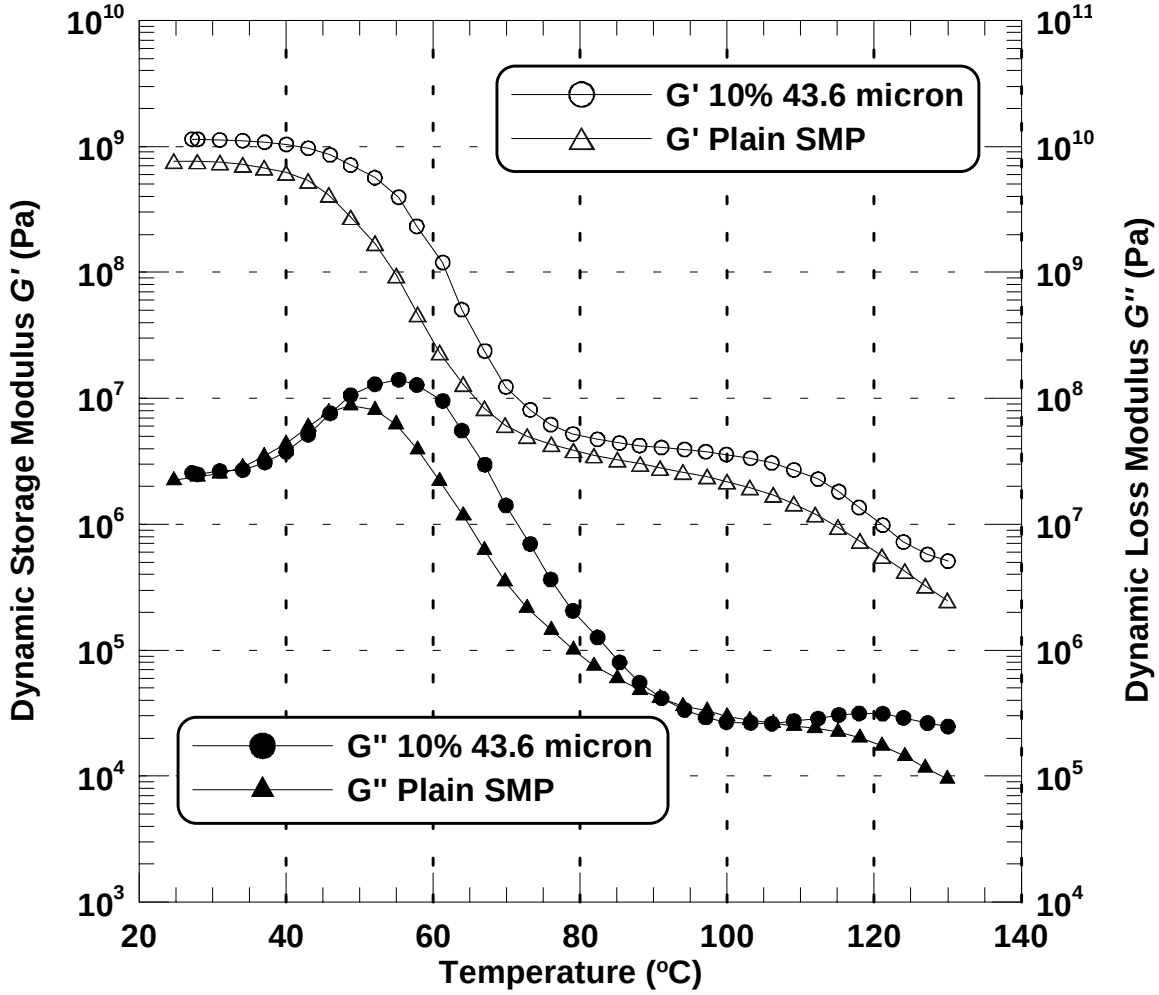
G' 10% 43.6 micron
G' Plain SMP
G'' 10% 43.6 micron
G'' Plain SMP
Dynamic Storage Modulus G' (Pa)
Dynamic Loss Modulus G'' (Pa)
Temperature (°C)
10^10
10^9
10^8
10^7
10^6
10^5
10^4
10^3
10^11
20
40
60
80
100
120
140

Fig. 7

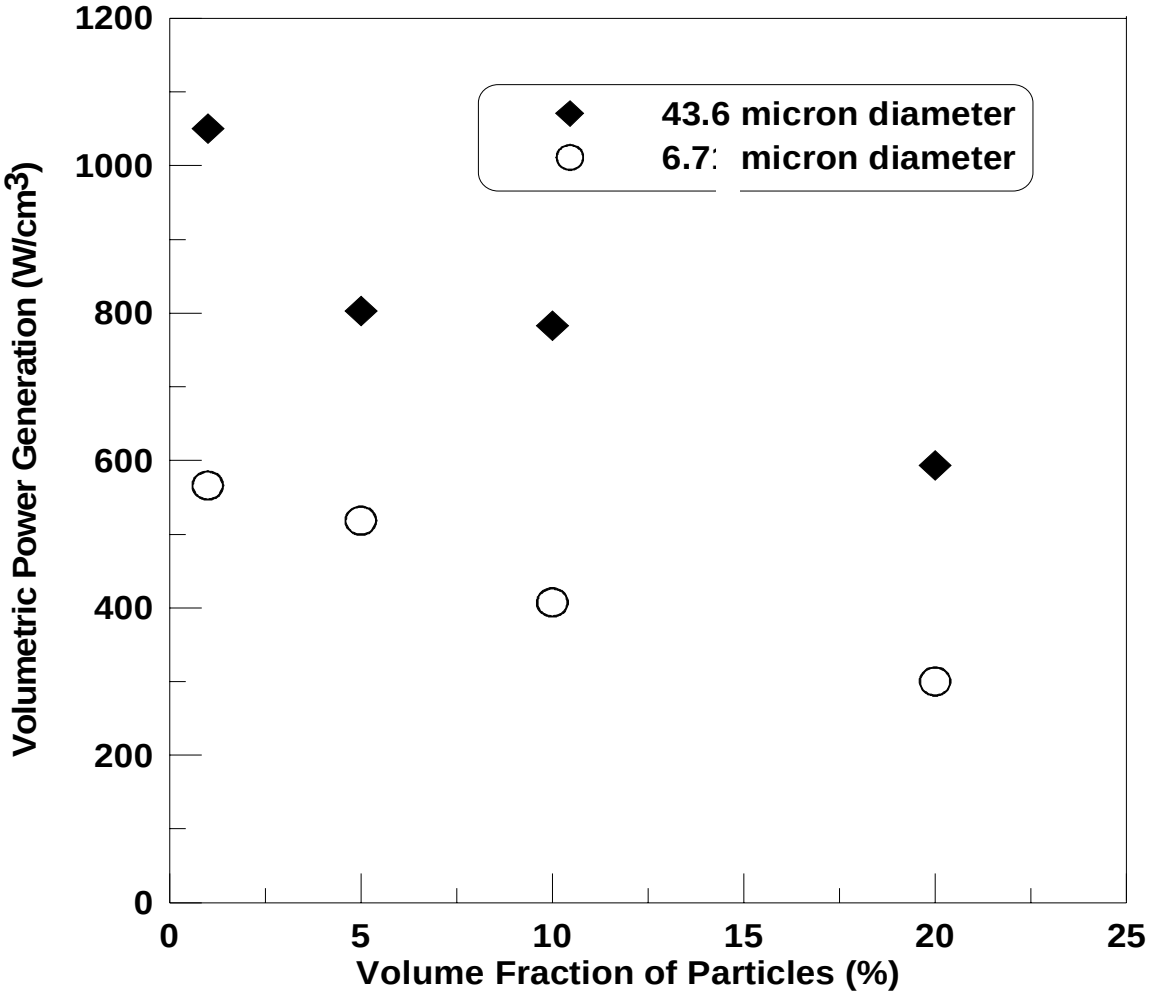

Fig. 8

FIGURE CAPTIONS

Fig 1. Effect of Zn substitution on the Curie temperature of NiZn ferrite [26].

Fig 2. Calibration curve (log fit to calculated data points) showing magnetic field generated at given power setting on Ameritherm Nova 1M equipment.

Fig 3. SMP devices used to evaluate feasibility of actuation by inductive heating. a) Flower shaped device shown in collapsed and actuated form. b) SMP foam device shown in collapsed and actuated form.

Fig 4. Calorimeter test setup with inductive coil specifications.

Fig 5. Heating curves of SMP loaded with 43.6 micron C2050 particles at varying volume contents with error bars at +/- one standard deviation. The slope of each curve was used to calculate the power dissipation.

Fig 6. a) Actuation of SMP flower shaped device with 10% volume fraction of 43.6μm particle diameter C2050 magnetic material (12.2 MHz at 400 A/m applied magnetic field). b) Actuation of SMP foam with 10% volume fraction of 43.6μm particle diameter C2050 magnetic material (12.2 MHz at 400 A/m applied magnetic field).

Fig 7. DMTA results for neat SMP and a 10% volume fraction of 43.6μm particle diameter C2050 magnetic material SMP sample.

Fig 8. Volumetric Power Dissipation of magnetic particles vs. Volume Fraction of Particles, 12.2 MHz and 545 A/m.

REFERENCES

[1] A. Lendlein and R. Langer, "Biodegradable, elastic shape-memory polymers for potential biomedical applications," *Science*, vol. 296, pp. 1673-1676, 2002.
[2] L. M. Schetky, "Shape Memory Alloys," *Scientific American*, vol. 241, pp. 74-82, 1979.
[3] M. V. Swain, "Shape Memory Behavior in Partially-Stabilized Zirconia Ceramics," *Nature*, vol. 322, pp. 234-236, 1986.
[4] K. Otsuka and C. M. Wayman, *Shape memory materials*. New York: Cambridge University Press, 1998.
[5] Y. Liu, K. Gall, M. L. Dunn, P. McCluskey, and R. Shandas, "Shape memory polymers for medical applications," *Advanced Materials and Processes*, vol. 161, pp. 31, 2003.
[6] M. Bertmer, A. Buda, I. Blomenkamp-Hofges, S. Kelch, and A. Lendlein, "Biodegradable shape-memory polymer networks: characterization with solid-state NMR," *Macromolecules*, vol. 38, pp. 3793-3799, 2005.
[7] A. Metcalfe, A.-C. Desfaits, I. Salazkin, L. H. Yahia, W. M. Sokolowski, and J. Raymond, "Cold hibernated elastic memory foams for endovascular interventions," *Biomaterials*, vol. 24, pp. 491, 2003.
[8] D. J. Maitland, M. F. Metzger, D. Schumann, A. Lee, and T. S. Wilson, "Photothermal properties of shape memory polymer micro-actuators for treating stroke," *Lasers In Surgery And Medicine*, vol. 30, pp. 1-11, 2002.
[9] M. F. Metzger, T. S. Wilson, D. Schumann, D. L. Matthews, and D. J. Maitland, "Mechanical properties of mechanical actuator for treating ischemic stroke," *Biomedical Microdevices*, vol. 4, pp. 89-96, 2002.
[10] H. M. Wache, D. J. Tartakowska, A. Hentrich, and M. H. Wagner, "Development of a polymer stent with shape memory effect as a drug delivery system," *Journal of Materials Science: Materials in Medicine*, vol. 14, pp. 109, 2003.
[11] K. Gall, C. M. Yakacki, Y. Liu, R. Shandas, N. Willett, and K. S. Anseth, "Thermomechanics of the shape memory effect in polymers for biomedical applications," *Journal of Biomedical Materials Research - Part A*, vol. 73, pp. 339, 2005.
[12] A. Goldman, *Modern ferrite technology*. New York: Van Nostrand Reinhold, 1990.
[13] P. Stauffer, T. Cetas, A. Fletcher, D. DeYoung, M. Dewhirst, J. Oleson, and R. Roemer, "Observations on the Use of Ferromagnetic Implants for Inducing Hyperthermia," *IEEE Transactions on Biomedical Engineering*, vol. 31, pp. 76-90, 1984.
[14] T. C. Cetas, E. J. Gross, and Y. Contractor, "A ferrite core/metallic sheath thermoseed for interstitial thermal therapies," *IEEE Transactions On Bio-Medical Engineering*, vol. 45, pp. 68-77, 1998.
[15] A. Jordan, P. Wust, H. Fahling, W. John, A. Hinz, and R. Felix, "Inductive heating of ferrimagnetic particles and magnetic fluids: physical evaluation of their potential for hyperthermia," *International Journal Of Hyperthermia: The Official Journal Of European Society For Hyperthermic Oncology, North American Hyperthermia Group*, vol. 9, pp. 51-68, 1993.

[16] W. Atkinson, I. Brezovich, and D. Chakraborty, "Usable Frequencies in Hyperthermia with Thermal Seeds," *IEEE Transactions on Biomedical Engineering*, vol. 31, pp. 70-75, 1984.
[17] J. A. Paulus and R. D. Tucker, "Cobalt Palladium Seeds for Thermal Treatment of Tumors Patent US5429583 issued July 4," 1995.
[18] N. Ramachandran and K. Mazuruk, "Magnetic microspheres and tissue model studies for therapeutic applications," in *Transport Phenomena In Microgravity*, vol. 1027, *Annals Of The New York Academy Of Sciences*, 2004, pp. 99-109.
[19] R. Hergt, W. Andra, C. d'Ambly, I. Hilger, W. Kaiser, U. Richter, and H.-G. Schmidt, "Physical Limits of Hyperthermia Using Magnetite Fine Particles," *IEEE Transactions on Magnetics*, vol. 34, pp. 3745-3754, 1998.
[20] A. E. Virden and K. O'Grady, "Structure and magnetic properties of NiZn ferrite nanoparticles," *Journal Of Magnetism And Magnetic Materials*, vol. 290, pp. 868-870, 2005.
[21] M. Ma, Y. Wu, J. Zhou, Y. Sun, Y. Zhang, and N. Gu, "Size dependence of specific power absorbtion of Fe3O4 particles in AC magnetic field," *Journal of Magnetism and Magnetic Materials*, pp. 33-39, 2004.
[22] Gray, Cammarano, and Jones, "Heating of Magnetic Materials by Hysteresis Effects Patent US659923B1 issued July 29, 2003." USA, 2003.
[23] A. Jordan, R. Scholz, P. Wust, H. Fahling, and F. Roland, "Magnetic fluid hyperthermia (MFH):Cancer treatment with AC magnetic field induced excitation of biocompatible superparamagnetic nanoparticles," *Journal of Magnetism and Magnetic Materials*, pp. 413-419, 1999.
[24] A. Jordan, R. Scholz, K. Maier-Hauff, M. Johannsen, P. Wust, J. Nadobny, H. Schirra, H.-G. Schmidt, S. Deger, S. Loening, W. Lanksch, and R. Felix, "Presentation of a new magnetic field therapy system for the treatment of human solid tumors with magnetic fluid hyperthermia," *Journal of Magnetism and Magnetic Materials*, pp. 118-126, 2001.
[25] J. Giri, A. Ray, S. Dasgupta, D. Datta, and D. Bahadur, "Investigation on T-c tuned nano particles of magnetic oxides for hyperthermia applications," *Bio-Medical Materials And Engineering*, vol. 13, pp. 387-399, 2003.
[26] X. K. Zhang, Y. F. Li, J. Q. Xiao, and E. D. Wetzel, "Theoretical and experimental analysis of magnetic inductive heating in ferrite materials," *Journal of Applied Physics*, vol. 93, pp. 7124-7126, 2003.
[27] A. Jordan, R. Scholz, P. Wust, H. Fahling, and R. Felix, "Magnetic fluid hyperthermia (MFH): Cancer treatment with AC magnetic field induced excitation of biocompatible superparamagnetic nanoparticles," *Journal Of Magnetism And Magnetic Materials*, vol. 201, pp. 413-419, 1999.
[28] V. Rudnev, *Handbook of induction heating*. New York: Marcel Dekker, 2003.
[29] Ameritherm, "Operation and Maintenance Instruction NovaStar 1M 10-15 MHz Power Supply, Doc # 801-9096 rC," Ameritherm Inc., Scottsville 2000.
[30] M. H. I. Ltd., "PROCESSING INSTRUCTIONS FOR SHAPE MEMORY POLYMER (Manual No.1 Rev. 2.2)," 1992.
[31] C. W. Macosko, *Rheology: principles, measurements, and applications*. New York: VCH, 1994.

[32] B. K. Kim, S. Y. Lee, and M. Xu, "Polyurethanes having shape memory effects," *Polymer*, vol. 37, pp. 5781-5793, 1996.
[33] L. H. Sperling, *Introduction to physical polymer science*. New York: Wiley, 1986.
[34] E. Wetzel and B. Fink, "Feasibility of Magnetic Particle Films for Curie Temperature-Controlled Processing of Composite Materials," Army Research Lab March 2001.
[35] C. Kittel, "Physical Theory of Ferromagnetic Domains," *Reviews of Modern Physics*, vol. 21, pp. 541-583, 1949.
[36] E. D. Bliznakov, C. C. White, and M. T. Shaw, "Mechanical properties of blends of HDPE and recycled urea-formaldehyde resin," *Journal of Applied Polymer Science*, vol. 77, pp. 3320-3227, 2000.